

Photonics for 5G

Antonella Bogoni, Luca Potì, Giancarlo Prati, Marco Romagnoli

Abstract Photonic technologies are largely used in optical communication systems and networks due to their unique characteristics in term of bandwidth, immunity to electromagnetic fields, compatibility with the optical fiber and flexibility. The possibility to fabricate photonic devices through CMOS compatible processes paves the way for low cost and reduced footprint circuits making optical technologies available for any network segments and new applications. Here the importance of Photonics for 5G development and deployment is addressed together with some technological alternatives and perspectives.

1 Optical systems enabling 5G

Antonella Bogoni
Scuola Superiore Sant'Anna - Pisa

Luca Potì
Photonic Networks & Technologies Nat'l Lab – CNIT, Pisa

Giancarlo Prati
Photonic Networks & Technologies Nat'l Lab – CNIT, Pisa
IRCPHoNeT, Pisa

Marco Romagnoli
Photonic Networks & Technologies Nat'l Lab – CNIT, Pisa

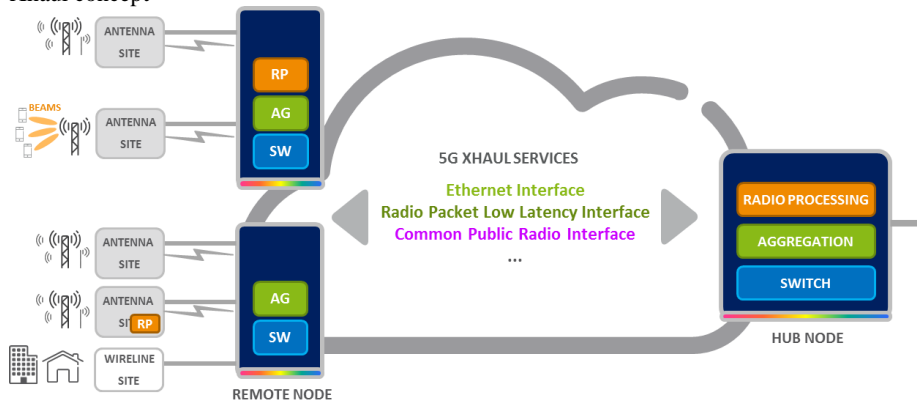
The rising penetration of smart connected devices, promising compelling services anywhere and anytime, is having a huge impact on the mobile broadband infrastructure and on the ability to provide a quality experience to the final users, whether humans or connected things. The new 5G radio access ecosystem, expected by 2020 [1], will have to sustain an average traffic increase of one order of magnitude and peak rates up to three orders of magnitude higher than the current ones [2]. Many time sensitive services will also demand extremely low transmission latency. Radio technologies will evolve by allocating new bands (beyond 10 GHz), by leveraging higher-order multiple-input multiple-output (MIMO), carrier aggregation, and beam forming techniques. In parallel, the transport network for backhaul (BH) and fronthaul (FH) applications will demand support of higher capacities to increase the number of transport clients, to support a wider range of performance requirements, and to provide increased flexibility. This must be achieved in a cost-effective and sustainable manner. Based on the radio architectures, it is possible to define many deployment scenarios, ranging from the fully centralized one, i.e., the cloud radio access network (CRAN), to the conventional scenario, in which all functions are replicated at each radio site with monolithic radio base stations (RBSs). Moreover, as envisioned in [3], novel radio-splitting models are under development to meet 5G high-bandwidth demands, leveraging different distributions of radio functions between radio unit nodes and centralized processing nodes. Realistic scenarios will see a mix of all mentioned radio architectures, with a combination of traffic types to be transported among the radio devices.

If mobile as communication was conceived for humans (mobile broadband and media delivery), 5G will include also machine type communication between devices (sensors, actuators etc.) that must communicate with the same wireless access technology. A vast variety of use cases are predicted for 2020 each with very different connectivity requirements: from the broadband access in a dense area or in a crowd, monitoring and automation of infrastructures and buildings, remote controlled heavy machines, control in real time of remote machines, intelligent transportation system, communication with high user mobility (500 Km/h), etc. as shown in Fig. 1.

Fig 1.
5G use cases



Fig 2.
Xhaul concept



The conventional point-to-point fronthaul concept is evolving towards a geographical network connecting a pool of DUs with a plurality of RRUs using the CPRI protocol (*Xhaul concept* shown in Fig. 2). Centralization of radio baseband processing functions is gaining great interest for its potential to allow a consolidation of nodes and network elements, so as to lower CapEx and OpEx (e.g. fewer nodes to install, to maintain, to upgrade, and to power supply), while at the same time increase radio coordination functions. Optical technologies with their conventional benefits of high bandwidth, protocol transparency, scalability, low latency, high resilience and network re-configurability, are today perceived as a promising key piece of the radio access network puzzle, in both fronthaul and backhaul transport areas. But previous generation of optical networking technologies (e.g. SDH/SONET, WDM, OTN etc.), based on discrete components

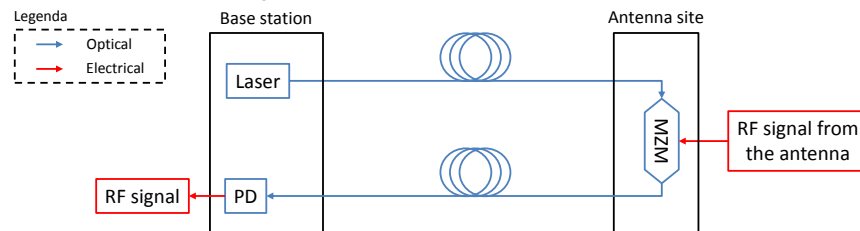
and modules, that played a relevant role to realize an affordable transport medium in metro and core networks are not adequate for the needs of the emerging RAN transport segments requiring low cost, lower power consumption and a level of miniaturization. Re-configurability features, provided by WDM technologies, can further increase CPRI transport efficiency.

However, to use WDM approach in radio access networks it is fundamental to dramatically reduce the cost figure of photonic components, modules, and sub-systems, with respect to corresponding ones that are today used in metro aggregation and long haul networks, to be acceptable in this portion of the network. Such a cost reduction must be achieved while re-shaping the performance of those ones. As an example, in a radio access network the transmission span ranges from few hundreds of meters up to few tens of Km, certainly not the several hundreds of Km that are required in metro and regional networks. On the other hand, in mobile fronthaul segments it is a must to comply with tight requirements in terms of latency, which could range in order of magnitude of hundreds or even tens of milliseconds. As a result, to adopt WDM technology in radio access and benefit of its peculiarities, it is necessary to reduce cost and re-shape performance of photonic technology. Photonic Integration and, in particular, silicon photonics with its recent advances in integrating many optical circuits and functions (for instance multiplexer, attenuator, switches, couplers) in a single chip using the well-developed CMOS production infrastructure, is the ideal technology to fit the RAN needs.

In addition, when an RF signal is loaded on an optical carrier, it becomes convenient to use optical fibers to transport the signal, implementing a *Radio-over-Fiber* (RoF) system. In fact, fiber transmission is broadband, low-loss (as low as 0.2 dB/km, while RF waveguides have a propagation loss in the order of several dB/m), and EMI free. Therefore, the optical fiber allows transporting the RF signal over long distances without significant distortions.

Considering the RoF system applied to a 5G radio system, the electro-optic and opto-electronic signal conversions can be realized by straightforwardly modulating the RF signal on an optical carrier at the optical transmitter side, and then detecting the optical signal in a wideband photodiode at the optical receiver side. If the fiber link is intended to remote a receiving antenna, as in the case of a radar system, it can be convenient to keep the laser at a base station, send the unmodulated optical carrier to the antenna through an optical fiber, and move to the antenna only an optical modulator, where the carrier is loaded with the received RF signal (Fig. 3) [4].

Fig 3.
Scheme of a RoF for remoting a receiver antenna.



A couple of possible issues arises with RoF solutions. The first one is related to the available linear dynamic range of the transport system, in fact the RoF systems using external optical amplitude modulation are often subject to nonlinearities induced by the modulator itself. In order to increase the maximum linear dynamic range, RoF systems exploiting phase modulation (PM) has been developed. While this kind of modulation is very linear, the opto-electronic conversion of the RF signal becomes more complex, requiring either a frequency discriminator for implementing a direct detection, or an even more complex coherent detection scheme [4]. A second issue is the effect of chromatic dispersion when the RF signal is transferred on the optical carrier by means of a double sideband (DSB) amplitude modulation. In fact, if the total chromatic dispersion of the fiber link is high enough (for example, due to a long fiber link), some frequency components of the two sidebands can undergo a significantly different phase shift due to the dispersion, which gives a notch in the transmissivity of the system at those frequencies that are turned exactly out-of-phase. In order to suppress the fading, it is possible either to make use of phase modulations, or to exploit the single sideband (SSB) amplitude modulation. Once the effect of the fading is suppressed, RoF systems can be used to cover spans as long as several hundred km, also thanks to the use of optical amplifiers (EDFAs).

Another application where optical technologies play a significant role is represented by *Optical beam forming*. The beam forming of RF signals in phased array antennas (PAAs, also called active electronically-steered antennas, AESAs) allows steering the transmitted RF beam without physically moving the antenna. This solution is used in wireless communications since it permits a strong reduction of size and weight in the antennas (no moving parts are needed!). It is a key functionality in 5G since next generation of mobile communication networks will guarantee high throughput to the users, relying on a better efficiency in

resources allocation and power consumption, with a more extended use of the frequency spectrum. User-specific beam forming (BF) will play a key role in the actualization of this strategy, especially in very crowded environments, where a precise steering and a fast re-orientation of the antenna beams are required [5].

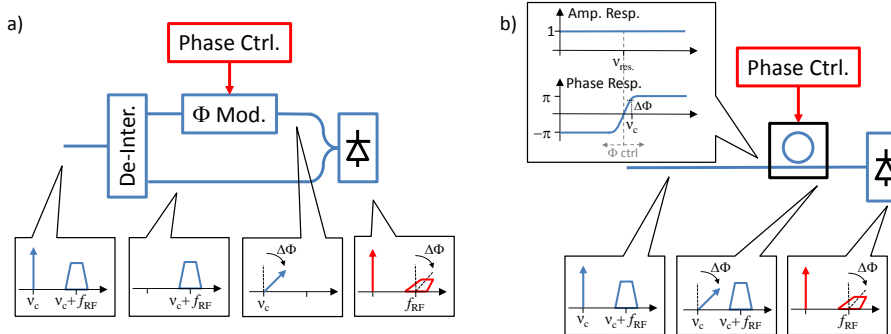
In the next-future mobile and wireless communications scenario, beam forming networks (BFNs) are expected to drive PAAs with potentially several elements, whose size will shrink due to the employed high frequency. Therefore, antenna pointing accuracy, low losses, reduced power consumption, and small size are crucial characteristics in future BFNs. In PAAs, the time of emission of the signal at each antenna element is controlled so that the wavefront of the signal generated by the entire antenna array is synthesized to propagate in the desired direction. The time of emission of the signal at each antenna element is commonly controlled by means of electronic phase shifters (PSs), since a phase shifting is a correct approximation of a time delay if the delay is small and the signal bandwidth is much narrower than the carrier frequency. In fact, under these hypotheses one can describe a time delay in terms of fractions of the carrier period. When the PAA is transmitting broadband signals, the approximation above does not hold anymore: in fact, in this case a constant phase shifting of all the spectral components in the broad signal spectrum would give different frequencies a different delay. Therefore, when the signal is broadband, the phase shifting approach induces a beam squinting: different frequencies of the signal spectrum aim at a different angle, losing directivity and gain in the antenna. In order to avoid it, a true time delay (TTD) must be controlled at each antenna element. In current electronically controlled PAAs, the phase shifting is realized by means of analog RF PSs. In case of broadband signals, instead, the TTD is implemented in the digital domain (rather than in the analog RF domain) by processing the numerical signal at each antenna element in order to synthesize a delay on the samples. This operation requires a huge digital processing capability, and is usually reserved for high-performance applications only.

In this perspective, photonics can provide promising solutions to meet the 5G requirements, potentially reducing also the cost of BFN elements, thanks to photonic integration [6], [7]. If the RF signal is transferred in the photonic domain, it is easy to implement either a phase shifting or a true time delay, taking advantage of the huge bandwidth, frequency flexibility, and EMI insensitivity of photonics. For both the PS and the TTD, several different solutions are available. In the following discussions, we will describe these methods considering the beam forming in transmission, but the same approaches can be used for controlling the

direction of detection in receiving PAAs. Let us consider an RF signal loaded on a laser by means of a single sideband modulation. To implement a phase shifting to the optically carried RF signal, it is necessary to shift the optical carrier with respect to the sideband. This way, once the optical signal is converted back to the RF domain by a photodiode, the variation in the phase difference between carrier and sideband is transferred to the RF signal. This can be realized by separating carrier and sideband in an optical de-interleaver (as the MRR-loaded MZ interferometer presented above), and shifting the carrier alone, e.g., in a phase modulator, before recombining the carrier and the sideband (Fig. 4a) [8],[9]. Another possible way for shifting the carrier only, is to use a wavelength specific phase shifter. For example, a microring resonator (MRR) under particular hypothesis on the coupling between the waveguide and the ring, realizes an all-pass filter that induces a 360° steep phase shift across its resonance wavelength. If the optical carrier is placed close to the MRR resonance, slightly changing the reciprocal position of the carrier and the microring will change the phase of the carrier without affecting the sideband (Fig. 4b) [10],[7]. These approaches can take advantage of the fast phase control ensured by the photonic techniques, so that phase tuning time faster than 1 ns can be achieved, regardless of the RF carrier frequency that can easily be as high as several tens of GHz.

Fig 4.

a) Phase shifting through de-interleaving and phase control; b) phase shifting through a wavelength-specific phase shifter, as a microring resonator in all-pass configuration.

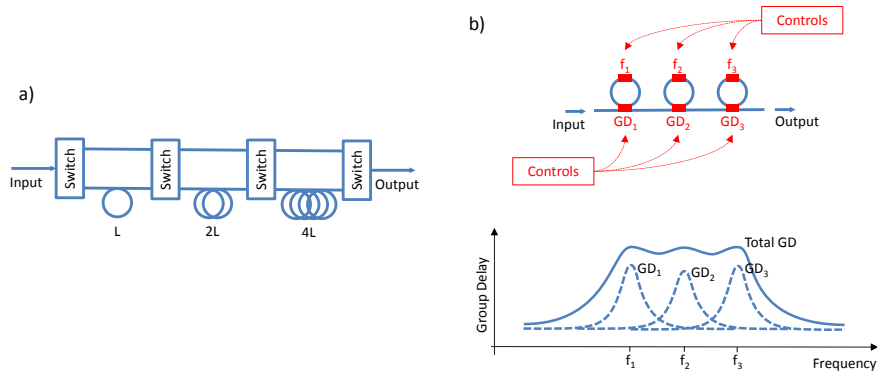


On the other hand, effective TTD based on photonics has been demonstrated exploiting several different approaches. The most straightforward one takes advantage of the low loss of optical waveguides to implement variable delays through optical path switching (Fig. 5a): the signal is switched among few optical

paths of different length, therefore with different propagation times [11]. A second type of TTD exploits the wavelength dependence of the laser propagation time through a medium due to the chromatic dispersion [11]-[14]: considering a modulated laser transmitted through, e.g., an optical fiber, if the laser wavelength is changed, the propagation time in the dispersive element changes as well. Therefore, it is possible to control the delay of an optical signal by controlling its wavelength. If the RF signal to each antenna element is loaded on an independent laser, by tuning the lasers it is possible to control the time of emission of the RF signal of every element in the array. For example, the dispersion-compensating fiber (DCF) has a dispersion of about -100 ps/nm·km; therefore, if a spool of 1 km is available, tuning the carrier wavelength of 1 nm will produce a variation in the time of arrival equal to 100 ps. Another relevant method for realizing a TTD using photonics exploits the so-called slow light effect, i.e., emulating the TTD by controlling the group delay of the optical sideband only [15]. This approach is based on the concept that the delay is the wavelength derivative of the phase; therefore, synthesizing phase variations with tunable steepness in the spectrum, it is possible to control the delay of the optical signal. An elegant implementation of this method has exploited the group delay of few cascaded optical micro-rings [16], controlling their resonance frequency through a phase control in the ring, and their group delay through the coupling between ring and waveguide (Fig. 5b). This last example is particularly significant since it has demonstrated a photonic-integrated beam forming network based on TTD for broadband signals at high frequency. The optical TTD is therefore an extremely interesting solution for high-performing beam forming. Nevertheless, its implementation is practically complex, in particular if tunable TTD is realized in integrated photonics, where several parameters must be controlled simultaneously at each antenna element. Therefore, if the target application does not make use of ultra-wideband signals, an approach based on optical phase shifting can be more convenient, trading off a limited amount of squinting with a significant simplification in the operational complexity [9].

Fig 5.

a) Photonics-based TTD based on path switching. b) Principle of wideband TTD based on group delay (GD) synthesis by MRRs.



2 Photonic technologies for 5G

5G wireless communication technology requires an increase in bandwidth of three orders of magnitude ($>500 \text{ Mb s}^{-1}$) for each user and all objects connected to the Internet, as the 5G evolution is driven by the growing mobile communication markets and the development of the Internet of Things (IoT). Therefore, there is urgent demand for technologies that can meet requirements in terms of bandwidth and power consumption. Photonics is poised to play an increasingly important role in ICT, since the fixed high capacity links are largely based on photonic technologies. At present, optical interconnections in data centres are mainly between boards that provide the platform on which the electronic components and optical or electro-optical devices are connected. In the near future, the number of optical interconnections will increase. As a result, by 2021, the production of optical interconnections is predicted to be >10 million per year. Photonic devices need to support ultra- large bandwidth operation, for example, 200 Tb s^{-1} in a single fibre and $>10 \text{ Tb s}^{-1} \text{ cm}^{-2}$ in integrated photonics chips. To achieve this, the key photonic components, e.g. photodetectors and modulators, need very high performances in terms of speed ($\geq 25 \text{ Gb s}^{-1}$), footprint ($<1 \text{ mm}^2$), insertion loss ($<4 \text{ dB}$), manufacturability ($>10^6$ pieces per year) and power consumption ($<1 \text{ pJ bit}^{-1}$). The photonic devices needed to meet these requirements are typically based on LiNbO_3 , III-V semiconductors such as InGaAsP/InP and semiconductors used in Silicon photonics. However, for technologies to become widespread, devices must be mass produced, cost efficient, reproducible, reliable, and compliant with

existing semiconductor processes and environmental regulations. With these considerations in mind, for large-scale production, Silicon photonics is preferable to others because the technological processes are the same as those already present in Si foundries commonly used in the semiconductor industry.

2.1 Silicon

Photonic Integrated Circuits (PICs) have become a commercial reality in a number of markets, especially in telecom and datacom. PICs enable complex optical and opto-electronic functions on a very compact footprint with high reliability. And because of wafer-scale manufacturing, the cost of a PIC can be significantly lower than with conventional technologies (relying on bulk optical or other assembly platforms) for the same function.

Silicon photonics is the field that takes advantage of more than 50 years of massive investment in silicon technology for electronic ICs. It leverages the vast know-how of the complementary metal-oxide-semiconductor (CMOS) world to develop PICs in the technologies of existing CMOS fabs. The field of silicon photonics has been growing at an amazing rate, both scientifically and industrially. Today more than 15 CMOS fabs (industrial fabs or semi-industrial R&D fabs) around the world have developed a mature process flow for silicon photonics. This allows to access a much larger scale of manufacturing with high volumes and low cost with respect to other technologies, e.g. Indium Phosphide.

Silicon photonics comprises passive and active optical devices and systems based on high refractive index Silicon or Silicon nitride waveguides which allow high-density integration of very compact devices including: high-speed phase modulators, phase shifters, switches, multiplexers, couplers, etc. Silicon photonics may include also other materials to provide functionalities not allowed by only Silicon, e.g. Germanium or III-V materials. Germanium is typically used to integrate photodetectors and electro-absorption modulators as it can be directly grown on Silicon and be processed in a CMOS line. III-V materials are used to integrate hybrid lasers or semiconductor optical amplifiers (SOAs) on Silicon, e.g. by wafer bonding or transfer printing techniques.

Silicon photonics is a key technology to satisfy the demanding challenges of next 5G networks: high bandwidth, low power consumption, small footprint. Silicon photonics optical interfaces have already reached high volumes for cloud data centers and have played an important role in mobile networking. As data rates of commercial optical interface increase from 10Gb/s to 25Gb/s, Silicon photonics will be even more critical to support high-speed, optical connectivity to/from cell tower. As an example, today Silicon Photonics supports the 100GbE optical interfaces with PSM4 and CWDM4 transceiver based on different standards. However, the 100GbE will soon evolve in 200GbE and 400GbE to increase the throughput of each module.

As examples of real devices a Silicon Photonics Optical Dispersion Compensator and an Optical Beam forming Networks are reported.

Example: Silicon Photonics Optical Dispersion Compensator

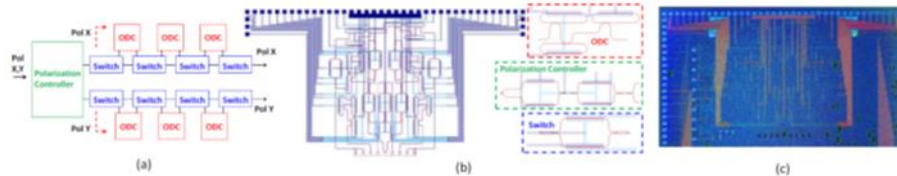
High speed optical direct detection (DD) interfaces based on DWDM technology could meet the needs of both emerging Cloud and 5G networks [17], provided that is possible to extend their distance reach up to 20 km. In this scenario, dispersion compensating devices based on integrated photonics, are appealing because they can be embedded in plug-and-play optical transceivers similar to the current Small Form Factor (SFP) modules. In [18] an integrated optical dispersion compensation module (ODCM) realized on a Silicon photonic (SiP) platform was presented. The SiP ODCM is able to receive and separate a polarization multiplexed (PolMux) signal in the C-band (ITU-T 100GHz DWDM grid), and compensates the chromatic dispersion accumulated up to 30km single mode fiber (SMF) transmission with a 10km granularity.

All-pass microring resonators have been demonstrated to be suitable for the design of optical dispersion compensators (ODC) [19]. An ODC for the compensation of the typical chromatic dispersion of a standard G.652 SMF at 1550nm is fabricated. The target SMF length is 10km with a constant-dispersion pass-band width of 50GHz. In order to obtain a flat group delay in the desired pass-band an ODC composed of three all-pass microring resonators was designed. The 10km ODC has been designed, on a SiP platform, defining the phase Φ , the power coupling ratio k and free-spectral range (FSR) of the three ring resonators [19]. The ODCM is equipped with a polarization active controller (PAC), based on a previously reported design [20], able to receive and separate the two polarizations of a PolMux signal into two independent sections of the module.

The two polarizations are then separately processed by two independent cascades of three 10km ODCs. Mach-Zehnder interferometer (MZI) based optical switches allows to select the number of 10km ODCs in which the signal will pass through on each arm, i.e. the SMF length to be compensated: 10km, 20km or 30km. Each of the employed all-pass ring resonators is equipped with an electric control in order to adjust the ODC response. Fig. 6 shows the ODCM schematic, the mask layout each building block and an optical microscope picture of the fabricated device.

Fig 6.

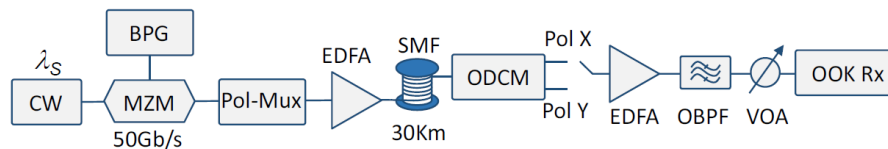
(a) Schematic of ODC module. (b) Mask layout of each building block. (c) Optical microscope picture of the fabricated device..



The fabricated ODCM was used in a transmission experiment to assess the expected extension of the optical reach. The experimental setup is shown in Fig. 7.

Fig 7.

Experimental setup for the transmission experiment and validation of the proposed ODCM

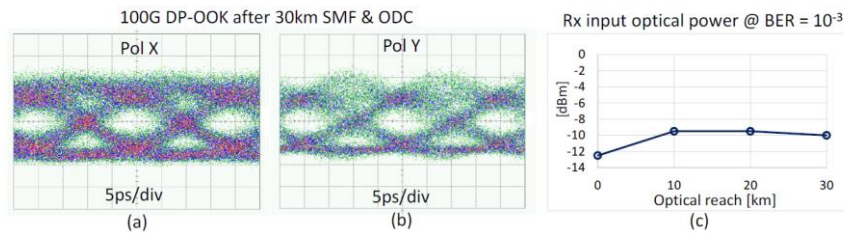


The light of a CW source is intensity modulated (IM) by a dual-drive Mach-Zehnder Modulator (MZM) driven by a 50Gb/s NRZ data stream ($2^{31}-1$ PRBS) generated by a programmable bit pattern generator (BPG). The available bit rate is doubled exploiting PolMux emulated through a split&delay PolMux emulator, obtaining a 100 Gb/s PolMux NRZ signal. The signal is then sent to different spools of G.652 SMF to assess the performance at different fiber lengths. At the receiver side, the incoming signal is coupled into the SiP ODCM through the dual polarization grating coupler of the PAC [4], which separates the two polarizations of the PolMux signal in the two arms of the SiP ODCM.

The two tributary signals at the output of the two arms are sent to an erbium doped fiber amplifier (EDFA) to compensate for the insertion losses of the chip which are larger than expected due to accidental fabrication impairments. The tributary signals are then sent to a DD NRZ Rx consisting of a 30GHz photodiode followed by a 50Gb/s symbol-by-symbol hard threshold detector. Fig. 8a and 8b show the eye diagrams for the two received polarizations after propagation over 30km of SMF and the ODCM. Transmission of the 100Gb/s PolMux NRZ signal over different SMF lengths, 10km, 20km and 30km was characterized by properly enabling the optical switches of the ODCM in order to process the signal with one, two or three 10km ODCs, respectively. To evaluate performance, the optical power required at the 50Gb/s DD NRZ receiver was measured for a pre-FEC BER = 10^{-3} , that is a typical reference value for hard-decision FEC with 7% overhead, suitable for Metro application. First the NRZ performance in back-to-back conditions was measured, where a BER = 10^{-3} was obtained with an optical power at the receiver of -12.5dBm. Then, the same measure was performed with different spools of standard G.652 fiber together with the ODCM. Fig. 5(c) shows the obtained pre-FEC sensitivity as a function of the transmission length. Results show a reasonable power penalty of 2.5dB at 30km, thus confirming the effectiveness of the ODCM to extend the optical reach of high bit rate IM/DD transmission in a metropolitan network scenario.

Fig 8.

(a) and (b): eye diagrams for the two received 50Gb/s polarizations after propagation over 30Km of SMF and chromatic dispersion compensation and polarization recovery in the ODCM. (c): optical power required at the direct detection OOK receiver as a function of the transmission length, for achieving a BER = 10^{-3} .



Example: Optical Beam forming Networks

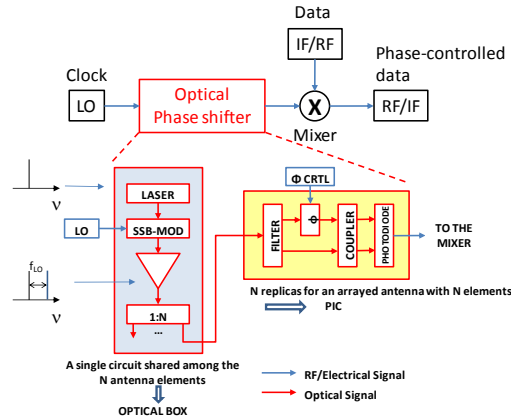
Optical phase shifting approach has been chosen, with respect to TTD, to minimize the impact of the optical solution on the standard radio board, guaranteeing at the same time, the main requirements for 5G . In fact, the additional broadening of the pointing beam originated by frequency-dependent response of a PS element is inversely proportional to the signal carrier frequency and to the number of array elements [21]. Thus, for small-to-moderate number of PAA elements (as in the case of cellular networks antennas), the squint-induced beam broadening can be considered a negligible fraction of the “natural” (i.e., in absence of modulation signal) beam width even for relatively large signal bandwidth and pointing angles, if the carrier frequency is sufficiently high. For instance, the calculated beam broadening due to squint effect for a 1D 8-element antenna array with a carrier frequency of 30 GHz and a 2 GHz signal bandwidth is less than 7° (for a natural beam width of 28.5°) for a pointing angle as large as 60° , and it reduces to $\sim 1^\circ$ (with the natural beam being $\sim 13^\circ$) when the pointing angle is 15° . In several 5G envisioned applications, small-size PAA with relatively limited scanning angles are expected to prove useful services, such as dynamic calibrations of the antenna line-of-sight between different stations. In general, since the 5G scenario will involve high bit rates and the envisaged carrier frequencies can be well beyond 30GHz, the PS approach might be justified by the strong reduction in the complexity and cost of the BFN architecture compared with the more performing TTD approach. The proposed solution aims at replacing the electrical phase shifter with an optical phase shifter as reported in Fig. 9.

The optical phase shifter includes to different blocks: the first one is shared among all the PAA elements and does not require photonic integration, while the second one is specific for each PAA element and should be integrated to reduce the footprint and the power consumption.

In the first block a continuous-wave laser (1558 nm) is modulated by a RF oscillator (13GHz) in a dual-nested Mach-Zehnder Modulator (DN-MZM), to obtain a single sideband optical signal. After amplification by an erbium-doped fibre amplifier (EDFA), the optical signal is split to the PSs in the BFN. The second block comprises an optical deinterleaver filter (ODF), an optical phase shifter (OPS), an optical coupler (OC), and a photodiode (PD). The operation of this clock relies on optical carrier-sideband separation performed by the ODF and subsequent phase shift of the isolated carrier in the OPS stage, before the two

components are recombined in the OC and sent to the PD to generate the phase-shifted microwave signal [22].

Fig 9.
OBFN architecture



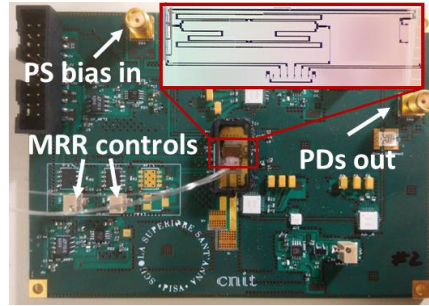
The phase of the down-converted signal at the PD output generated by the beating between the carrier and the sideband components is indeed given by the phase difference of the two beating signals. Assuming a perfect carrier-sideband isolation at the ODF outputs, the amount of optical phase shift ϕ experienced by the optical carrier in the OPS translates into an equal phase shift ϕ of the microwave signal at f_{RF} without any amplitude modulation. The PSs are all calibrated to centre the filtering port of the DI to the laser wavelength.

This second scheme has been realized in SOI technology which simultaneously matches the demand for wide phase-shift range, broad bandwidth, low in-band power oscillations, fast (i.e., sub- μ s) reconfiguration speed, and compatibility with CMOS integrated circuits fabrication technology. The phase modulator is realized as a reverse-biased Si p-n junction, while the ODF is implemented by a micro ring resonator (MRR)-loaded Mach-Zehnder interferometer structure.

The photonic integrated circuit (PIC) is able to perform stable phase shifts well in excess of 360° over a bandwidth of 6 GHz for RF carriers spanning in the X, Ku, an mm-wave bands, with limited in-band power variations of ~ 1 dB, and small response time below 1 ns. A picture of one PS element composed of the PIC and its driving circuitry is shown in Fig. 10.

Fig 10.

Picture of the photonics-based PS, with the PCB (printed circuit board) hosting the PIC.
Inset: Microscope picture of the PIC



The photonics-based BFN has been characterized for a 4-element PAA. We analysed the static and dynamic behavior of the RF beam controlled by the BFN. The main specifications are reported in Table 1. The OBFN works at 13 GHz and all odd multiples, due to the periodical behavior of the ODF, with a bandwidth >400 MHz. The use of photonic integration introduces high losses (10 dB), reducing the power efficiency. However, the faster (<1 ns compared to the state of the art value $> \mu$ s) and more precise ($<1^\circ$ compared to the state of the art value $> 4^\circ$) beam steering guaranteed by the photonics-based phase shifters makes this approach a promising solution to BF for PAAs in future 5G networks.

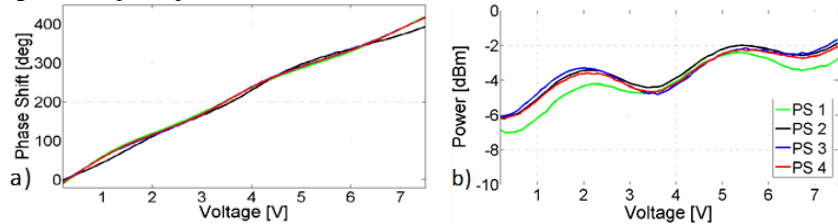
RF frequency	13 GHz and odd multiples
Phase precision	0.06 deg/mV
Response time	<1 ns
3-dB bandwidth	400 MHz
PIC loss (including 4 dB for coupling)	10 dB
Total RF loss	40 dBm
Output RF power	-40 dBm

Table 1: OBFN specifications

For the static characterization, power and phase responses of each PS element are measured on a vector network analyser while gradually changing the DC voltage applied to the phase modulator in the PIC. The results are reported in Fig. 11. Fig.

11a shows the phase shift produced on the 13 GHz output RF signal by each PS. The 4 curves exhibit a good linearity, with a phase variation in excess of 360° over less than 7 V. Fig. 11b shows the power fluctuations induced on the RF signal by varying the control voltage: a power variation within ~ 4 dB is measured over a 360° phase shift. In fact, a change in the polarization of the p-n junction induces a change in its refractive index, i.e. on its transparency. This entails a variation of the attenuation of the optical signal propagating through the phase modulator; hence, the RF power variation. In the following power variations effect on the beam emitted by a PAA is considered.

Fig 11. Characterization of the phase shift (a) and output power (b) of the 4 PSs, versus the applied voltage to the optical phase modulator.

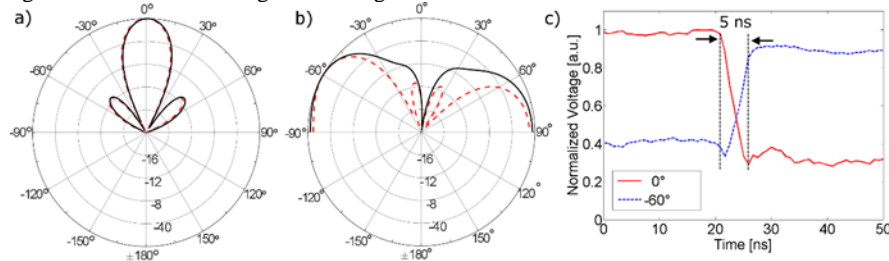


The radiation pattern of a PAA can be obtained by multiplying the radiation pattern of the single element with the array factor $AF(\theta)$ [23]. Considering four antenna elements spaced by $\lambda/2$, the AF diagram of an ideal PAA pointing at 0° can be calculated as reported by the dashed red line in Fig. 12a. Instead, the AF of the photonics-based BFN is calculated by measuring on the oscilloscope the relative amplitude and actual phase shifts $\Delta\theta_n$ of each PS, for a steering angle $\theta_0 = 0^\circ$. The obtained AF is represented by the solid black line of Fig. 12a). As expected, the ideal and real AFs coincide. Then, the phase settings are changed for pointing at $\theta_0 = -60^\circ$. The calculated AF is reported in Fig. 12b) compared with the ideal one. The curves for the ideal and real AF are in good agreement, both showing the maximum at -60° , but a difference in the shape can be recognized. This is due to the optical power fluctuations in the PSs studied in Fig. 12b). A modification of the PIC is already under study to suppress these fluctuations and hence improve the beam forming accuracy of the BFN. In the dynamic characterisation, the PSs are driven to simultaneously switch between the phase settings $\theta_0 = 0^\circ$ and $\theta_0 = -60^\circ$; their outputs are acquired by a real-time oscilloscope and processed. The red solid curve in Fig. 12c) shows the RF power

behaviour seen from the view angle $\theta = 0^\circ$ during the steering from 0° to -60° , while the blue dashed curve reports the RF power observed at the same time from the view angle $\theta = -60^\circ$. The power behaviour clearly describes the effective steering of the PAA, changing quickly from a static condition at $\theta = 0^\circ$ to a static condition at $\theta = -60^\circ$. The power levels seen from $\theta = 0^\circ$ and -60° are not equal, as it would be expected, due to the power fluctuations discussed above. The time needed by the BFN to switch the beam between the two angles is about 5 ns, in line with the requisites for reconfiguring PAAs in 5G networks. The switching time of the bare PIC was previously estimated in ~ 1 ns. As a fact, the measured 5 ns is limited by the bandwidth of the available step-function generator (80 MHz) used for controlling the PSs, confirming the estimation of the previous analyses.

Fig 11.

Comparison of ideal (dashed red lines) and real (solid, black lines) array factor diagrams for a PAA pointing at 0° (a) and at -60° (b). (c): Power emitted by the PAA as seen from view angles at 0° and -60° during the steering switch.

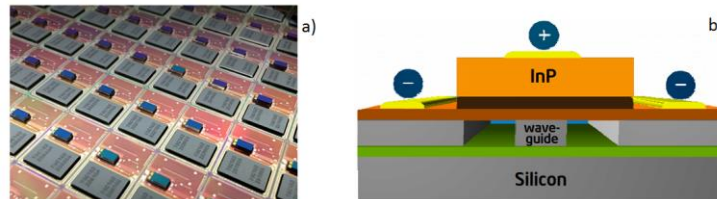


2.2 Hybrid integration and innovative technologies

Silicon photonics enables the integration of many optical functions on a chip allowing compactness, low cost and large scale of manufacturing. However, Silicon is an indirect bandgap semiconductor, i.e. it is not suitable for optical amplification and lasing. Today the most straightforward method to integrate laser sources with Silicon photonics is co-packaging of separate chips, i.e. the Silicon photonics PIC and the laser, inside a single package, as shown in Fig. 12. This approach has the advantage to exploit at maximum the different technologies, but at the same time introduces some drawback, e.g. in terms of compactness and extra losses due to optical interfacing of the two worlds.

Fig. 12

a) Co-packaged multi-chip: Silicon PIC, silicon EIC and laser [23]. b) Wafer bonded laser [24].



The integration of lasers and optical amplifiers is also possible by heterogeneous integration of Silicon photonics and III-V semiconductor technologies. The hybrid integration of III-V semiconductor optoelectronic components onto Silicon photonics PICs can be obtained in different ways, as for example flip-chip integration, hetero-epitaxial growth, wafer bonding or transfer printing.

Flip-chip integration has the advantage that the devices are fabricated on their III-V native substrate and then glued on the Silicon photonics PIC, which requires accurate alignment in the assembly process. The hetero-epitaxial growth approach allows for front-end, wafer-scale integration of the III-V materials, however it is quite difficult to obtain high quality materials. Wafer bonding approaches combine some of the advantages of flip-chip integration because the III-V material is grown on its native substrate and then bonded on Silicon, with the manufacturability of wafer-scale integration as the device fabrication is finalized on the Silicon photonics process flow. The transfer printing approach is an alternative bonding technology offering some advantages. The devices are partially processed on the native substrates and then transferred using a PDMS stamp to the target Silicon photonic PIC.

Hybrid integration of laser sources with Silicon photonics is currently developed in commercial 100GbE Silicon photonics modules ready to support next 5G wireless Radio Access Network (RAN) fronthaul. Hybrid integration of semiconductor optical amplifiers (SOAs) is also very important to develop low loss optical networks. A lot of effort is spent worldwide for the integration of III-V SOAs on complex Silicon Photonic switching matrix.

At present, among the established technologies the most promising is Silicon Photonics. However, to date, the requirements of the next 5G network seem to be not fulfilled in just one system. New materials have emerged to expand the functionalities of current technologies with better performance in terms of efficiency and cost. Graphene photonics is emerging as an innovative solution

fully compatible with Silicon Photonics and able to improve the performance of current Silicon photonics devices.

Graphene is an allotrope of Carbon in which Carbon atoms are arranged in a single atom thick hexagonal lattice, i.e. a 2D material. Graphene exhibits peculiar optoelectronic properties and can be used for light modulation and photodetection. Graphene-based integrated photonics for high-speed datacom and telecom applications have been demonstrated [24]. Graphene-based photodetectors integrated on Silicon Photonics already reached good responsivities and operation bandwidth. Graphene-based modulators have been demonstrated to provide advantages over Si- based modulators. They are capable of broadband electro-absorption and electro-refraction operation with improved efficiency with respect to the standard Silicon Photonics platform.

Graphene devices are compatible with complementary metal oxide semiconductor (CMOS) processing, and enable post-processing fabrication and the use of different substrates. Graphene devices have also the advantage that does not require implantations on Silicon or Germanium hetero-epitaxy. Hence, the waveguide can be Silicon, Silicon Nitride, Silica or another transparent material. Practically, this implies a post-processing shift in manufacturing from front-end to back-end-of-line. In addition, Graphene technology does not necessarily require expensive SOI wafers, or implantation for junctions, and Ge growth for detectors. Because SiN and SiO₂ waveguides are wider than Si photonics ones, the lithography node can be relaxed. The waveguide size is $\sim 0.5 \mu\text{m}$ for Si, $\sim 1.5 \mu\text{m}$ for SiN and $\sim 8 \mu\text{m}$ for SiO₂. All these factors will simplify the technology and reduce costs.

References

1. NGMN, "5G White Paper," Feb. 2015 [Online]. Available: https://www.ngmn.org/uploads/media/NGMN_5G_White_Paper_V1_0.pdf.
2. [2] Ericsson, "Ericsson Mobility Report," Nov. 2015 [Online]. Available: <http://www.ericsson.com/res/docs/2015/mobilityreport/> ericsson-mobility-report-nov-2015.pdf.
3. Ericsson, "Cloud RAN," White Paper, Sept. 2015 [Online]. Available: <https://www.ericsson.com/res/docs/whitepapers/wp-cloud-ran.pdf>.

4. J. Beas, G. Castanon, I. Aldaya, A. Aragon-Zavala, G. Campuzano, "Millimeter-wave Frequency Radio over Fiber Systems: A Survey", *IEEE Commun. Surveys Tuts.*, v.15, n.4, 2013
5. A. Osseiran, et al., "5G Mobile and Wireless Communications Technology", Cambridge University Press, June 2016.
6. L. Zhuang, et al., "Novel ring resonator-based integrated photonic beamformer for broadband phased array receive antennas-Part II: Experimental prototype", *Journ. Lightwave Technol.*, 28 (1), 2010, pp. 19-31.
7. D.B. Adams, and C.K. Madsen, "A Novel Broadband Photonic RF Phase Shifter", *J. Lightwave Technol.*, 26 (15), 2008, pp. 2712-2717.
8. G. Serafino, C. Porzi, V. Sorianoello, P. Ghelfi, A. D'Errico, S. Pinna, M. Puleri, M. Romagnoli, A. Bogoni, "Design and Characterization of a Photonic Integrated Circuit for Beam Forming in 5G Wireless Networks", MWP 2017.
9. F. Falconi, C. Porzi, S. Pinna, V. Sorianoello, G. Serafino, M. Puleri, A. D'Errico, M. Romagnoli, A. Bogoni, P. Ghelfi, "Fast and Linear Photonic Integrated Microwave Phase-Shifter for 5G Beam-Steering Applications", OFC 2018.
10. M. Pu, L. Liu, W. Xue, Y. Ding, H. Ou, K. Yvind, and J. M. Hvam, "Widely tunable microwave phase shifter based on silicon-on-insulator dual-microring resonator", *Optics express*, 18(6), 2010, pp. 6172-6182.
11. R. Soref, "Optical dispersion technique for time-delay beam steering", *Applied Optics*, vol. 31, no. 35, pp. 7395-7397, 1992.
12. L. Yaron, R. Rotman, S. Zach, M. Tur, "Photonic Beamformer Receiver With Multiple Beam Capabilities", *IEEE Photonics Technology Letters*, vol. 22, no. 23, pp. 1723-1725, 2010.
13. K. Prince, M. Presi, A. Chiuchiarelli, I. Cerutti, G. Contestabile, I.T. Monroy, E. Ciaramella, "Variable Delay With Directly-Modulated R-SOA and Optical Filters for Adaptive Antenna Radio-Fiber Access", *IEEE Journal of Lightwave Technology.*, vol 27, no. 22, pp. 5056-5064, 2009.
14. F. Scotti, P. Ghelfi, F. Laghezza, G. Serafino, S. Pinna, A. Bogoni, "Flexible True-Time-Delay Beamforming in a Photonics-Based RF Broadband Signals Generator," *IET Conference Proceedings*, pp. 789-791, 2013.
15. A. Zadok, O. Raz, A. Eyal, M. Tur, "Optically Controlled Low-Distortion Delay of GHz-Wide Radio-Frequency Signals Using Slow Light in Fibers", *IEEE Photonics Technology Letters*, vol. 19, no. 7, pp. 462-464, 2007.
16. A. Meijerink, C.G. Roeloffzen, R. Meijerink, L. Zhuang, D.A. Marpaung, M.J. Bentum, M. Burla, J. Verpoorte, P. Jorna, A. Hulzinga, W. Van Etten, "Novel Ring Resonator-Based Integrated Photonic Beamformer for Broadband Phased Array Receive Antennas—Part I: Design and Performance Analysis", *IEEE Journal of Lightwave Technology*, vol. 28, no. 1, pp. 3-18, 2010.
17. X. Liu et al., "Emerging optical access network technologies for 5G wireless," *IEEE/OSA Journal of Optical Communications and Networking*, vol. 8, no. 12, pp. B70-B79 (2016).
18. V. Sorianoello, G. De Angelis, F. Fresi, F. Cavaliere, L. Poti, M. Midrio, and M. Romagnoli, "100Gb/s PolMux-NRZ Transmission at 1550nm over 30km Single Mode Fiber Enabled by a Silicon Photonics Optical Dispersion Compensator," in *Optical Fiber Communication Conference, OSA Technical Digest (online) (Optical Society of America, 2018)*, paper W2A.31.
19. C. K. Madsen et al., "Integrated all-pass filters for tunable dispersion and dispersion slope compensation," *IEEE Photonics Technology Letters*, vol. 11, no. 12, pp. 1623-1625 (1999).

20. P. Velha et al., "Wide-band polarization controller for Si photonic integrated circuits", *Opt Lett.* 41(24), pp. 5656-5659 (2016).
21. Hansen, Robert C. *Phased array antennas*. Vol. 213. John Wiley & Sons, 2009.
22. V.J. Urick et al., "Microwave phase shifting using coherent photonic integrated circuits", *IEEE J. Sel. Topics Quant. El.*, vol. 22, no. 6, Dec. 2016.
23. F. Amato et al., "Ultra-fast Beam Steering of a Phased-Array Antenna Based on Packaged Photonic Integrated Circuits" in *Proc. ECOC2018, Rome, Italy, Spet. 2018*.
24. <http://www.luxtera.com/silicon-photonics-technology/>
25. Intel. *A Hybrid Silicon Laser Silicon photonics technology for future tera-scale computing*, White Paper. (2006)
26. M. Romagnoli, et al., Graphene-based integrated photonics for next-generation datacom and telecom, *Nat. Rev. Materials* vol. 3, pp. 392-414 (2018)